THE PROPERTIES OF SPUTTERED COPPER OXIDE THIN FILM FOR SENSING APPLICATION

LOW JIA WEI

A thesis submitted in
fulfilment of the requirements for the award of the
Degree of Master of Electrical Engineering with Honors

PTTA UTHM
PERPUSTAKAAN TUNKU TUN AMINAH

Faculty of Electrical and Electronic Engineering
Universiti Tun Hussein Onn Malaysia

MAC 2015

ABSTRACT

Gas sensor is an important functional device that will guarantee the safety of human from being exposed to hazardous gases. The important features of a gas sensor are the ability to response towards the gas at the shortest time, the sensitivity towards the specific gas and the portability of gas sensor device. In this thesis, the optimum parameters required to deposit CuO thin film for gas sensing application using RF magnetron sputtering was investigated by correlating the copper oxide plasma and thin film. The optimum oxygen flow rate for the deposition of CuO thin film was observed to be 8sccm base on the ratio of copper and oxygen emission obtained from the OES analysis. Moreover, through the XRD analysis it was confirmed that pure CuO compound was formed at above 8sccm oxygen flow rate. As for the substrate bias voltage, the ideal value was -40V base on the ion flux value obtained through Langmuir probe analysis. In addition, comparison on the topography, morphology, roughness and sheet resistance at various substrate bias voltages through FE-SEM, AFM and two-point-probe analysis help confirmed the structure that were suitable for gas sensing application. Besides, the sheet resistance of the CuO thin film that were deposited at -40V substrate bias voltage and 8sccm oxygen flow rate was near to $10^6\Omega$ which is close to fully oxidized copper oxide thin film. Lastly, a simple experimental setup was constructed to test the functionality of the CuO thin film as a gas sensor.

PTTA UTHM PERPUSTAKAAN TUNKU TUN AMINAH

ABSTRAK

Sensor gas adalah sejenis alat yang sangat penting untuk menjamin keselamatan manusia daripada terdedah kepada gas-gas berbahaya. Ciri-ciri penting dalam sensor gas adalah keupayaan untuk bertindak balas terhadap gas pada masa yang singkat, kepekaan terhadap gas yang tertentu dan kemudahalihan peranti sensor gas. Dalam thesis ini, parameter optimum yang diperlukan untuk untuk fabrikasi kuprum oksida (CuO) sensor gas applikasi menggunakan radio frekuensi (rf) *magnetron sputtering* telah disiasat dengan menghubungkaitkan plasma dan filem nipis kuprum oksida. Kadar aliran oksigen yang optimum untuk fabrikasi CuO filem nipis telah diperhatikan pada 8sccm berdasarkan pada nisbah kuprum dan oksigen pancaran yang diperolehi melalui spektroskopi pemancaran optic (OES). Selain itu, ia telah disahkan melalui analisis XRD bahawa sebatian CuO tulen telah dibentuk pada kadar aliran oksigen 8sccm. Manakala, bagi voltan pada sample, nilai ideal adalah sebanyak -40V berdasarkan nilai fluks ion yang diperolehi melalui analisis *Langmuir probe.* Di samping itu, perbandingan struktur, permukaan, kekasaran dan *sheet* rintangan pada voltan sampel yang berbeza melalui analisa *FE-SEM*, *AFM* dan *two-point-probe* telah mengesahkan struktur yang sesuai untuk aplikasi sensor gas. Selain itu, *sheet* rintangan daripada CuO filem nipis yang difabrikasikan pada -40V voltan pada sampel dan kadar aliran oksigen 8sccm adalah berhampiran dengan $10^6\Omega$ iaitu ia menunjukkan kuprum oksida tersebut telah hamper teroksida dengan sepenuhnya. Akhir sekali, eksperimen yang ringkas telah disediakan untuk menguji fungsi filem nipis CuO sebagai gas sensor

CONTENTS

	TITLE	**i**
	DECLARATION	**ii**
	DEDICATION	**iii**
	ACKNOWLEDGEMENT	**iv**
	ABSTRACT	**v**
	CONTENTS	**vii**
	LIST OF TABLES	**x**
	LIST OF FIGURES	**xi**
	LIST OF SYMBOLS AND ABBREVIATIONS	**xvii**
CHAPTER 1	**INTRODUCTION**	**1**
	1.1 Problem Statements	3
	1.2 Aim and Objective	4
	1.3 Scopes	4
CHAPTER 2	**LITERATURE REVIEW**	**5**
	2.1 Background	5
	2.2 Gas sensor development	6
	2.3 Copper oxide gas sensor	7
	2.4 Sputtering plasma deposition	9
CHAPTER 3	**RESEARCH METHODOLOGY**	**11**
	3.1 Introduction	11
	3.2 Gas sensor fabrication	13
	3.3 In-situ and ex-situ analysis	17
	3.4 Gas sensor testing	28

PTTA UTHM
PERPUSTAKAAN TUNKU TUN AMINAH

CHAPTER 4 IN-SITU ANALYSIS DURING THE FABRICATION OF COPPER OXIDE THIN FILM **33**

4.1 Introduction 33

4.2 Optical emission of Cu, Ar and O in magnetron sputtering plasma 34

4.3 Plasma characteristic of magnetron sputtering plasma 44

4.4 Conclusion 54

CHAPTER 5 EX-SITU ANALYSIS OF COPPER OXIDE DEPOSITION AT VARIOUS PARAMETERS **55**

5.1 Morphological properties of deposited copper oxide thin film 56

5.2 Topography of deposited copper oxide thin film 64

5.3 Structural properties of deposited copper oxide thin film 70

5.4 Electrical properties of copper oxide thin film 75

5.5 Conclusion 79

CHAPTER 6 GAS SENSING PERFORMANCE OF COPPER OXIDE THIN FILM SENSOR **81**

6.1 Time response analysis 84

6.2 Recovery time analysis 86

6.3 Conclusion 87

CHAPTER 7 CONCLUSION **88**

7.1 Strength and significance of this work 89

7.2 Future work 90

REFERENCES **91**

APPENDIX **101**

LIST OF PAPERS **105**

PTTA UTHM PERPUSTAKAAN TUNKU TUN AMINAH

LIST OF TABLES

2.1	Specifications of CuO doped SnO_2 and ZnO gas sensor	8
2.2	Specification of homogeneous CuO gas sensors	8
2.3	A compilation of various techniques used to deposit copper oxide as the gas sensing material	10
3.1	The deposition conditions of the prepared copper oxide thin films	17
4.1	Optimized point for the oxygen flow rate for various substrate bias voltage to produce CuO thin film	42
4.2	Electron density value of the Cu plasma at various oxygen flow rate and substrate bias voltage	47
4.3	Ion density value of the Cu plasma at various oxygen flow rate and substrate bias voltage	50
4.4	Plasma potential value of the Cu plasma at various oxygen flow rate and substrate bias voltage	51
4.5	Debye length value of the Cu plasma at various oxygen flow rate and substrate bias voltage	53
4.6	Ion flux value of the Cu plasma at various oxygen flow rate and substrate bias voltage	54
5.1	Thickness of copper oxide thin film deposited at various oxygen flow rate and substrate bias Voltage	63

PTTA UTHM PERPUSTAKAAN TUNKU TUN AMINAH

5.2	Surface roughness of copper oxide thin films at various oxygen flow rate and substrate bias voltage	69
5.3	Grain size of copper oxide thin films at various oxygen flow rate and substrate bias voltage	75
5.4	The sheet resistance for copper oxide thin film fabricated at various oxygen flow rate and substrate bias voltage	79
6.1	Time response for each of the parameters	85
6.2	Recovery time for all the parameters	87

PTTA UTHM
PERPUSTAKAAN TUNKU TUN AMINAH

LIST OF FIGURES

3.1	Flow chart of the process for fabricating the copper oxide gas sensor	12
3.2	Gas sensor schematic diagram	12
3.3	An internal view of the furnace	14
3.4	A schematic diagram of RF magnetron sputtering	15
3.5	A general scheme of magnetron discharge	15
3.6	Thickness against deposition time of copper oxide thin films prepared at 5, 10, 15 and 20minutes	16
3.7	The OES result for the He-Ne laser radiation	19
3.8	The actual result obtainable from the Ocean Optics Spectra Suite software	19
3.9	RF magnetron sputtering embedded with OES	20
3.10	Probe tip assembly in the Hiden Analytical ESPion system	21
3.11	RF magnetron sputtering embedded with Langmuir probe.	21
3.12	The initial variable setting available in the Hiden Analytical Software Suite.	22
3.13	The appearances of the Hiden Analytical Software Suite before analysis.	22
3.14	FE-SEM schematic diagram	24
3.15	Schematic diagram of an AFM	25
3.16	Simple X-ray diffraction schematic design	27
3.17	Typical I-V characteristic curve	28
3.18	Experimental setup for the two point probes	28
3.19	The schematic diagram of the circuit design	29

PTTA UTHM PERPUSTAKAAN TUNKU TUN AMINAH

3.20	An overview of the gas sensor circuit design	29
3.21	Experimental setup for the gas sensor testing	30
3.22	Actual arrangement of the gas sensing experimental setup	30
3.23	Chamber design with $2.01 x 10^{-3} m^3$ in volume	31
3.24	An overview of the gas chamber	31
3.25	A simple illustration of the experiment	32
4.1	The typical OES result during Ar and Ar + O emission environment	35
4.2	The oxygen emission at wavelength 777nm	35
4.3	Copper emission at various oxygen flow rate and substrate bias voltage	37
4.4	Oxidation reaction of copper in reactive magnetron sputtering	37
4.5	Argon emission at various oxygen flow rate and substrate bias voltage	40
4.6	Oxygen emission at various oxygen flow rate and substrate bias voltage	40
4.7	Normalized intensity for oxygen and copper emission at (a)0V, (b)-40V, (c)-60V and (d)-100V substrate bias voltage.	42
4.8	Normalized intensity for oxygen and copper emission at (a)8sccm and (b)16sccm oxygen flow rate	43
4.9	Typical result for Langmuir probe	45
4.10	The plot of Ion current versus probe voltage	46
4.11	The plot of $\ln(I_e)$ versus probe voltage	46
4.12	Electron density resulting from sputtering plasma of Cu under various oxygen flow rate and substrate bias voltage	47
4.13	Electron temperature of the plasma at various oxygen flow rate and substrate bias voltage	49

PTTA UTHM
PERPUSTAKAAN TUNKU TUN AMINAH

4.14	Ion density distribution resulting from sputtering plasma of Cu under various oxygen flow rate and substrate bias voltage	49
4.15	Plasma potential resulting from sputtering plasma of Cu under various oxygen flow rate and substrate bias voltage	51
4.16	Debye length resulting from sputtering plasma of Cu under various oxygen flow rate and substrate bias voltage	52
4.17	Ion flux resulting from sputtering plasma of Cu under various oxygen flow rate and substrate bias voltage	53
5.1	FE-SEM image of the copper oxide thin film deposited at -0V substrate bias voltage and (a) 0sccm, (b) 4sccm, (c) 8sccm and (d) 16sccm oxygen flow rate	57
5.2	FE-SEM image of the copper oxide thin film deposited at -40V substrate bias voltage and (a) 0sccm, (b) 4sccm, (c) 8sccm and (d) 16sccm oxygen flow rate	59
5.3	FE-SEM image of the copper oxide thin film deposited at -60V substrate bias voltage and (a) 0sccm, (b) 4sccm, (c) 8sccm and (d) 16sccm oxygen flow rate	60
5.4	FE-SEM image of the copper oxide thin film deposited at -60V substrate bias voltage and (a) 0sccm, (b) 4sccm, (c) 8sccm and (d) 16sccm oxygen flow rate	62
5.5	The graph of thickness versus oxygen flow rate	63
5.6	The graph of deposition rate versus oxygen flow rate	64

PTTA UTHM
PERPUSTAKAAN TUNKU TUN AMINAH

5.7	AFM image with line profile of the copper oxide thin film deposited at 0V substrate bias voltage and (a) 0sccm, (b) 4sccm, (c) 8sccm and (d) 16sccm oxygen flow rate	65
5.8	AFM image with line profile of the copper oxide thin film deposited at -40V substrate bias voltage and (a) 0sccm, (b) 4sccm, (c) 8sccm and (d) 16sccm oxygen flow rate	66
5.9	AFM image with line profile of the copper oxide thin film deposited at -60V substrate bias voltage and (a) 0sccm, (b) 4sccm, (c) 8sccm and (d) 16sccm oxygen flow rate	67
5.10	AFM image with line profile of the copper oxide thin film deposited at -100V substrate bias voltage and (a) 0sccm, (b) 4sccm, (c) 8sccm and (d) 16sccm oxygen flow rate	68
5.11	The graph of surface roughness versus oxygen flow rate	69
5.12	XRD spectra for substrate bias voltage -0V at various oxygen flow rate	71
5.13	XRD spectra for substrate bias voltage -40V at various oxygen flow rate	72
5.14	XRD result for substrate bias voltage -60V at various oxygen flow rate	73
5.15	XRD spectra for substrate bias voltage -100V at various oxygen flow rate	74
5.16	Structural composition of the dominant copper oxide element	74
5.17	I-V characteristic of the copper oxide thin films at 0sccm oxygen flow rate	77
5.18	I-V characteristic of the copper oxide thin films at substrate bias voltage -0V	77

PTTA UTHM
PERPUSTAKAAN TUNKU TUN AMINAH

5.19	I-V characteristic of the copper oxide thin films at substrate bias voltage -40V	78
5.20	I-V characteristic of the copper oxide thin films at substrate bias voltage -60V	78
5.21	I-V characteristic of the copper oxide thin films at substrate bias voltage -100V	79
6.1	Gas sensing performance for the copper oxide thin films deposited at substrate bias voltage -0V	82
6.2	Gas sensing performance for the copper oxide thin films deposited at substrate bias voltage -40V	82
6.3	Gas sensing performance for the copper oxide thin films deposited at substrate bias voltage -60V	83
6.4	Gas sensing performance for the copper oxide thin films deposited at substrate bias voltage -100V	83
6.5	The graph of time response versus oxygen flow rate	85
6.6	The graph of recovery time versus oxygen flow rate	86

PTTA UTHM
PERPUSTAKAAN TUNKU TUN AMINAH

LIST OF SYMBOLS AND ABBREVIATIONS

V_P	-	Plasma Potential
T_e	-	Electron Temperature
λ_D	-	Debye Length
n_i	-	Ion Density
n_e	-	Electron Density
d	-	Distance
Θ	-	Bragg angle
λ	-	Wavelength
V_{OUT}	-	Output Voltage
R_P	-	Potentiometer
Rsensor	-	Sensor Resistance
V_S	-	Voltage Source
M	-	Ion Mass
I_{esat}	-	Electron Saturation Current
A_P	-	Probe Area
W	-	Work Function
E_{VAC}	-	Near Surface Vacuum Energy
E_F	-	Fermi Level Energy
E_{EA}	-	Electron Affinity
E_C	-	Near Surface Conduction Band Edge
V	-	Voltage
SnO_2	-	Tin dioxides
Al_2O_3	-	Aluminum Oxide
Bi_2O_3	-	Bismuth Oxide
CdO	-	Cadmium Oxide
CeO_2	-	Ceria

PTTA UTHM PERPUSTAKAAN TUNKU TUN AMINAH

Cr_2O_3	-	Chromium Oxide
Co_3O_4	-	Cobalt Oxide
CuO	-	Copper (II) oxide or Cupric Oxide
Fe_2O_3	-	Iron Oxide
Ga_2O_3	-	Gallium Oxide
In_2O_3	-	Indium Oxide
MoO_3	-	Molybdenum Oxide
Nb_2O_5	-	Niobium Oxide
NiO	-	Nickel Oxide
WO_3	-	Tungsten Oxide
V_2O_5	-	Vanadium Oxide
ZnO	-	Zinc Oxide
Cu_2O	-	Copper (I) oxide or Cuprous Oxide
CO_2	-	Carbon Monoxide
VOC	-	Volatile Organic Compound
OES	-	Optical Emission Spectroscopy
AFM	-	Atomic Force Microscope
FE-SEM	-	Field Emission Scanning Electron Microscope
XRD	-	X-Ray Diffraction
RF	-	Radio Frequency
SiO_2	-	Silicon Dioxide
O	-	Oxygen
Ar	-	Argon
DC	-	Direct Current
Cu	-	Copper
PSPD	-	Position-Sensitive Photo Detector
Au	-	Gold
He	-	Helium
Ne	-	Neon
Kr	-	Krypton
Xe	-	Xenon
3D	-	Three Dimensional

PTTA UTHM
PERPUSTAKAAN TUNKU TUN AMINAH

CHAPTER 1

INTRODUCTION

Semiconducting metal oxide gas sensors currently establish as one of the most investigated group of gas sensors. It have been known for a long time that electrical resistance of a semiconductor is very sensitive to the changes on the surface [1]. Among the sensors investigated and developed, semiconducting metal oxide attracts much attention in the field of gas sensing under atmospheric conditions due to their low cost, flexibility in production, simplicity of their use and most important is that it detect large number of gases [2]. Recently, numerous researchers have shown interest in the characteristics of metal oxide semiconducting to tune its ability to produce a reaction with gases on the surface [3]. However, the reaction between the gas and solid-state metal oxide semiconducting often influenced by several factors such as internal and external changes towards the surface of the sensor. Some of the internal influences are related to the basic properties of the material used, surface areas and microstructure of the sensing layers. As for the external influences, they are caused by change in the temperature and humidity of the atmosphere.

The gas sensor can be defined as a tool that converts chemical energy into an electrical signal. Basically, the output signal is exhibited in the form of resistance changes [4]. Depending on the type of semiconductor metal oxide used, n-type semiconductor will have a decreased in the material resistance when alcohol is used as the sensing target (instead of increasing in the case of p-type semiconductor) [5]. The basic operation of a gas sensor is due to the absorption of oxygen on the crystal surface with a negative charge. Upon contact, the donor electrons in the crystal surface are transferred to the adsorbed oxygen, resulting in leaving positives charges in a space charge layer. Thus, surface potential is formed and act as a potential

PTTA UTHM PERPUSTAKAAN TUNKU TUN AMINAH

barrier against electron flow. At grain boundaries, absorbed oxygen forms a potential barrier which prevents carrier from moving freely. Hence, the electrical resistance of the sensor is increased. In the presence of a reducing gas, the surface density of the negatively charged oxygen decreases, so the potential barrier decreases and thus the sensor resistance also decreased. The reason that the negatively charged oxygen decreases is due to the reaction between the reducing gases with oxygen [6].

A great deal of efforts has been put into developing new sensing materials with improved sensor properties. Metal oxides possess a broad range of electrical, chemical and physical properties that are often highly sensitive to changes in their chemical environment. Because of these properties, metal oxides have been widely studied. Since the first semiconductor gas sensor was created in 1960's, various types of semiconducting metal oxide have emerge including SnO_2, TiO_2, Al_2O_3, Bi_2O_3, CdO, CeO_2, Cr_2O_3, Co_3O_4, CuO, Fe_2O_3, Ga_2O_3, In_2O_3, MoO_3, Nb_2O_5, NiO, WO_3 and V_2O_5 [4]. A wide range of sensing gas that were investigated include H_2S, NH_3, CH_4, CO, CO_2, H_2, NO, O_2, C_2H_5OH, and acetone. Basically, CuO is commonly used as an additive to enhance the gas sensor response of common metal oxide such as SnO_2 and ZnO [7–9]. Therefore, the suitability of CuO as homogeneous sensing material is one of the on-going research problem and in this thesis we have tried to optimise the oxygen flow rate and substrate bias voltage during the deposition of CuO thin film using RF magnetron sputtering.

Copper oxide (CuO) is a very interesting material for gas sensor due to its low cost material, excellent reactivity and nontoxicity [10]. Other than that, the benefit of using copper oxide as the gas sensing material is due to the initial material copper, Cu, natural abundance, easiness to produce Cu oxidation, non-toxic nature and realistically good electrical properties [11–13]. To date, various type of CuO thin film based gas sensors have been previously fabricated by the chemical vapor deposition [14], microwave-assisted hydrothermal [15], reactive DC sputtering [16] and RF magnetron sputtering [17]. So far, CuO thin film based gas sensor was used to detect NO_2, CO_2, CO, H_2S, NH_3, methanol and ethanol. In this case, ethanol will be the targeted type of gas sensing due to it's being categorized as one of the volatile organic compound (VOC) [18].

There have been reports of some interesting work based on CuO thin film by A. S. Zoolfakar *et. al.* [17]. Although the work about CuO thin film prepared by RF magnetron sputtering method is impressive and show very good response towards

PTTA UTHM PERPUSTAKAAN TUNKU TUN AMINAH

12.5ppm of ethanol. However, the sensing is observed at 180ºC operating temperature. In addition to this, there are no detailed reports on ethanol sensing using copper oxide thin films without operating temperature.

In our present work, the detailed study is performed on the correlation of in-situ and ex-situ analysis of the RF magnetron sputtered copper oxide thin film for ethanol by varying the oxygen flow rate and substrate bias voltage. In addition to this, we are presenting the copper oxide thin films for gas sensing application operated without heating element. In order to check the functionality of the copper oxide thin film, all the observations are done at least 3 times.

1.1 Problem Statements

Volatile organic compounds (VOCs) emitted from poultry production are leading source of air quality problems. VOC can be caustic and hazardous colourless gas with a characteristic pungent odour. VOC is present in animal waste and in particularly high concentration in chicken faeces. In Malaysian livestock industries, where chicken can live in unventilated environments, VOC concentration can become high enough to create illness to chicken and kill the animals. Recent example of this problem is the bird nest industries where the Chinese government bans the bird nest import from Malaysia. This was due to high compound of ammonia in Malaysia's bird nest. Therefore, an ability to monitor and control these environments is highly desirable.

Ethanol vapour, as one of the VOCs, has been one of the most thoroughly studied gases for gas sensor [5, 19, 20], particularly due to it being volatile, flammable and colourless liquid. Besides, ethanol is the principal type of alcohol found in alcoholic beverages. Nevertheless, ethanol can cause intoxication when consumed in sufficient quantity.

One of the major roles of nanotechnology in agriculture is to develop an autonomous sensor for air quality real-time monitoring linked to GPS. Nanotechnology will create a precision farming and thus maximize the output while minimizing input. The existing VOC sensor uses tin oxide or tungsten oxide semiconductor as the sensing elements requires high current for heating element and high concentration of VOCs. Therefore, it is not suitable for remote farming in

PTTA UTHM PERPUSTAKAAN TUNKU TUN AMINAH

Malaysia. High power consumption creates extra electrical works and cost which is not practical for small and medium enterprise (SME).

Even though there is a lot of type of gas sensor available in the market, but most of the available gas sensor required either a large volume of gas before the gas sensor activated or it required heating the gas sensor in order to be activated when in contact with low volume of gas. Other than that, the disadvantage of current gas sensor is that it is not suitable for mobile sensing system and it requires high power consumption. Therefore, in this project a high sensitivity copper oxide based gas sensor will be investigated and developed.

1.2 Aim and Objective

The aim of this project is to develop a CuO thin film for gas sensing application.

The objectives of this research include:

i. Deposition of CuO thin film using RF magnetron sputtering method.
ii. Correlation of copper oxide plasma and thin film analysis.
iii. Test the CuO thin film for gas sensing application.

1.3 Scopes

The main scope of this project is to investigate and deposit a CuO thin film for gas sensing application. The scopes include:

1. To investigate the plasma properties during the growth of copper oxide thin film at various oxygen flow rate and substrate bias voltage by using optical emission spectroscopy and Langmuir probe techniques.
2. To investigate the properties of copper oxide thin film deposited at various oxygen flow rate and substrate bias voltage by using FE-SEM, AFM, XRD and two point probe.
3. To deposit copper oxide thin film for ethanol gas sensing application.
4. To propose the optimized parameter to deposit CuO thin film for gas sensing application using magnetron sputtering technique.

PTTA UTHM PERPUSTAKAAN TUNKU TUN AMINAH

CHAPTER 2

LITERATURE REVIEW

2.1 Background

Agriculture is one of the main industrial in Malaysia which consists of cultivation of animals, plant and other life form for food, biofuel and other product to enhance human life. As one of the backbone for Malaysia, agriculture is the essential element for the developing countries, with more than 60% of the population reliant on it for their livelihood [21]. Therefore, uncontrolled environmental surrounding the industrial poultry production is related with the health risks for both animals and employees of the poultry industry [22]. Under industrial poultry production, it is often associated with the emissions of volatile organic compounds (VOCs) that lead to air quality problems. VOC is a caustic and hazardous colorless gas with a characteristic pungent odor. Therefore, a high concentration of VOCs from the livestock building may create illness to chicken or even kill the animals. VOC is present in animal waste and in particularly high concentration in chicken faeces. In livestock industries, where chicken can live in unventilated environments, VOC concentration can become high enough to create illness to chicken and kill the animals. In general, an uncontrolled emission of VOCs will lead to health problem on people living. Hence, an ability to monitor and control the emission is highly desirable.

On July 2011, there was issue on the quality of birds' nest imported to China after the Chinese authorities found that the quality of the birds' nest did not fulfill the permissible nitrite level. Based on the investigation, it was believe that the red coloured nest or cave nest was found to contain more than 1000ppm level of nitrite

PTTA UTHM PERPUSTAKAAN TUNKU TUN AMINAH

which was unsafe for human consumption [23]. Thus, there was a requirement for research to improve the quality of the birds' nest.

On April 2012, 24 workers at the Petronas gas processing plant in Kertih were admitted to hospital with breathing difficulties caused by a gas leakage. The gas believed to be ammonia [24]. Besides than agriculture, VOCs such as ammonia is also commonly found in gas processing plant and refrigerator as a coolant. In a different case, six people died from inhaling ammonia that leaked from a faulty refrigeration system at a jetty in Kampung Bagan Pasir which occur on 2009 [25].

One of the major roles of nanotechnology in agriculture and oil and gas industries is to develop an autonomous sensor for air quality real-time monitoring. Nanotechnology will create a precision analysis on the current working environment. Nanotechnology would possibly help to detect a small amount of VOC at very low power (or current) input. Therefore, such VOC sensor will be suitable for remote farming in Malaysia as well as remote oil drilling plant. High power consumption creates extra electrical works and cost which is not practical for small and medium enterprise (SME).

2.2 Gas sensor development

The major development of gas sensor has been directed into three types; with the first type is the potentiometric gas sensor, the second type is the calorimetric gas sensor and the third type is chemiresistive gas sensor. Basically, potentiometric gas sensor and calorimetric gas sensor are more specific in detecting oxygen and inflammable gases, respectively [4]. However, this thesis will be focusing on the third type, chemiresistive gas sensor, due to the nature of the gas to be investigated. The gas that was used in this investigation is the volatile organic compound gas which is commonly found in the agriculture development area. As one of the volatile organic compound, ethanol gas will be the main concern in this work.

Ethanol gas is one of the most comprehensively studied gases for gas sensing application [19]. This is because ethanol gas sensors are extensively used in the field of wine quality monitoring, breath analysis and particularly on food industries [17]. Other than that, ethanol gas can cause intoxication when consumed in sufficient quantity. Therefore, ethanol gas sensor has become crucial part of devices to our human society. As human life becomes more convenient, we are exposed to

PTTA UTHM PERPUSTAKAAN TUNKU TUN AMINAH

uncountable threats from the environment. In 2013, Chinese government bans the bird nest import from Malaysia due to high compound of ammonia (NH_3 is one of the VOCs) in Malaysia's bird nest. Even though gas sensor have being introduced for a long period of time but the sensitivity of the gas sensor towards low concentration of gases is still unsatisfied. Now, gas sensors are easily found in our daily life, from house to car and even the breath analyzer for drunken driver etc.

In poultry industry, many kinds of emission from various sources such as faeces of animals will cause the hazardous gas to increase. Some gases might be harmful to our health but they might not be noticeable at low concentration due to it to be odorless. Among those commercialized gas sensors, most of the gas sensor wan incorporated with heating element. Heating element is commonly used to regulate the operating temperature of the sensor. Applying heating element on the sensor will increase the sensitivity of the sensor towards the target gas [26]. Thus, this type of gas sensor increases the power consumption. Due to higher consumption of power, this type of gas sensor is not encouraged to be used at rural area due to unstable supply of electricity. With this idea, the aim in this thesis is to produce a gas sensor that will provide high sensitivity towards VOCs while removing the heating element usage from the devices itself. Therefore by removing the heating element, the power consumption from the devices will be much lower and it will be suitable to be used as a mobile sensing device.

2.3 Copper oxide gas sensor

Copper oxide oxide (CuO and Cu_2O) are important p-type semiconductors that have being widely investigated for various applications such as dye sensitized solar cell, photo catalysis, photochromic devices and last but not least the gas sensing devices. As an important p-type semiconductor, copper oxide have drawn numerous attention in the application of gas sensors due to its low cost material, excellent reactivity and nontoxicity [10]. Other than that, the benefit of using copper oxide as the gas sensing material is due to the initial material copper, Cu, natural abundance, easiness to produce Cu oxidation, non-toxic nature and realistically good electric properties [11–13].

Copper forms two type of oxides which is called cuprous oxide (Cu_2O) and cupric oxide (CuO). Due to the natural properties of nanostructured metal oxide films,

PTTA UTHM PERPUSTAKAAN TUNKU TUN AMINAH

tremendous efforts have taken places to develop copper oxide into various morphologies, such as cubes, wires, spheres etc. In fact, it is well known that nanostructured metal oxide films exhibit large surface area to volume ratio and this bring contribution to obtaining higher sensitivity gas sensor and rapid response. Based on these, numerous researchers have put a lot of efforts into investigating and improving the properties of copper oxide. Basically, CuO is a common material that is used as additive in order to improve the sensitivity and selectivity of SnO_2 and ZnO. Table 2.1 is a summary of reports on improvement in gas sensing when CuO is used as a dopant for SnO_2 and ZnO. Table 2.2 shows the sensing gas capability of homogeneous CuO gas sensor.

Table 2.1: Specifications of CuO doped SnO_2 and ZnO gas sensor.

Sensing Element	Target Gas	Operating Temperature(ºC)	Reference
SnO_2 - CuO	H_2S	300-400	[27, 28]
ZnO - CuO	NH_3	100-350	[29, 30]

Table 2.2: Specification of homogeneous CuO gas sensors.

Target Gas	Operating Temperature(ºC)	Reference
Acetone	220	[10, 12]
CO	200	[31, 32]
CO_2	160	[16, 33]
Ethanol	160-300	[5, 15]
Methanol	220	[5, 10]
N_2	200	[16, 34]

PTTA UTHM PERPUSTAKAAN TUNKU TUN AMINAH

2.4 Sputtering plasma deposition

Throughout this year, different techniques were used to fabricate nanostructured copper oxide as a gas sensing material for various types of target gases such as acetone, CO, CO_2, ethanol, H_2S, Methanol, N_2 and NH_3. Some of the known techniques to fabricate nanostructured copper oxide include chemical vapor deposition [12], microwave-assisted hydrothermal [15], reactive DC sputtering [16] and RF magnetron sputtering [17]. In this thesis, the copper oxide thin film will be prepared using RF magnetron sputtering technique.

W. R. Grove was the first person to study what became known as ‘sputtering’ at 1852 whereas others had observed the effect while studying glow discharges. Since that most of the physical vapour deposition is closely associated with the development of vacuum technology, the first piston type vacuum pump was invented by Otto van Guericke at 1640 in order to pump water out of mines. However, the first person to apply the vacuum pump in order to form a glow discharge in a ‘vacuum tube’ was M. Faraday in 1838. Since then, magnetron sputtering was studied by several researcher and the first uses of radio frequency (RF) to sputter material was investigated in the 1960s.

In 1966, Davidse and Maiseel used RF sputtering to produce dielectric films from dielectric materials. However, RF sputter deposition is not used widely due to their high cost and the introduction of high temperatures, due to the high self-bias voltage associated with RF power. RF sputtering was then developed to sputter deposited hard coatings on tools at mid-1970s and became commercially available at early 1980s [35]. Magnetron sputtering is a technique that requires a high energy of ions for bombardment, amounting to a few hundred of electron volts around the cathode. Due to the bombardment of the ions towards the cathode, fast metal atoms are formed along with secondary electrons. Basically, during the sputtering process, gas ions at the plasma were accelerated towards the target material that to be deposited. The material will then detached from the target and deposited on the substrate.

Basically, the advantages of reactive sputtering compared to chemical vapor deposition, reactive DC sputtering and microwave–assisted hydrothermal techniques is due to reactive sputtering deposit thin film at low deposition rates and the oxygen content can be controlled to produce specifically only CuO. Beside of CuO, Cu_2O

PTTA UTHM PERPUSTAKAAN TUNKU TUN AMINAH

and pure Cu composition will also exist on the thin film depending on the amount of oxygen content. However, Cu_2O and pure Cu composition can be avoided by gaining the knowledge on the plasma and thin film. Other than that, varying the substrate bias voltage during the deposition of thin film is also one of the main concerns on this experiment. Table 2.3 is the compilation of some of the techniques used to fabricate copper oxide sensing material.

Table 2.3: A compilation of various techniques used to deposit copper oxide as the gas sensing material.

Technique	Sensing material	Type of gas detected	References
Reactive DC sputtering	CuO	CO_2, Methanol, Ethanol	[5, 16]
Chemical Vapor Deposition	Cu_2O, CuO	Acetone, Ethanol	[12, 14]
Microwave-assisted hydrothermal	CuO nanorods, CuO nanoparticles	Ethanol, Methanol, Acetone	[10, 15]
RF magnetron sputtering	Cu_2O, CuO	Ethanol	[17, 36]

PTTA UTHM PERPUSTAKAAN TUNKU TUN AMINAH

CHAPTER 3

RESEARCH METHODOLOGY

3.1 Introduction

In this experiment, RF magnetron sputtering technique was used to fabricate copper oxide thin film. During the process, the plasma produced during sputtering will also be analyzed using optical emission spectroscopy (OES) and Langmuir probe. While the thin film will be analyzed using surface analysis equipment's such as field emission scanning electron microscope (FE-SEM), atomic force microscope (AFM), X-Ray diffraction (XRD) and two point probe. The correlation between plasma and thin film analysis will be used as a reference to produce an optimized condition in order to develop a CuO based gas sensor. The standardized process to analyzed and fabricate the copper oxide based gas sensor was according to the flow chart in figure 3.1.

The fabricated copper oxide thin films were constructed to form a gas sensor device which consists of 4 different layers, as shown in figure 3.2. The first layer of the gas sensor device is the Si substrate. This is because in this thesis, p-type Si wafer were used. As for the second layer, it is the SiO_2 layer which act as the insulator for this gas sensor. The main function for an insulator is to prevent leakage current from copper oxide thin film [37, 38].

PTTA UTHM PERPUSTAKAAN TUNKU TUN AMINAH

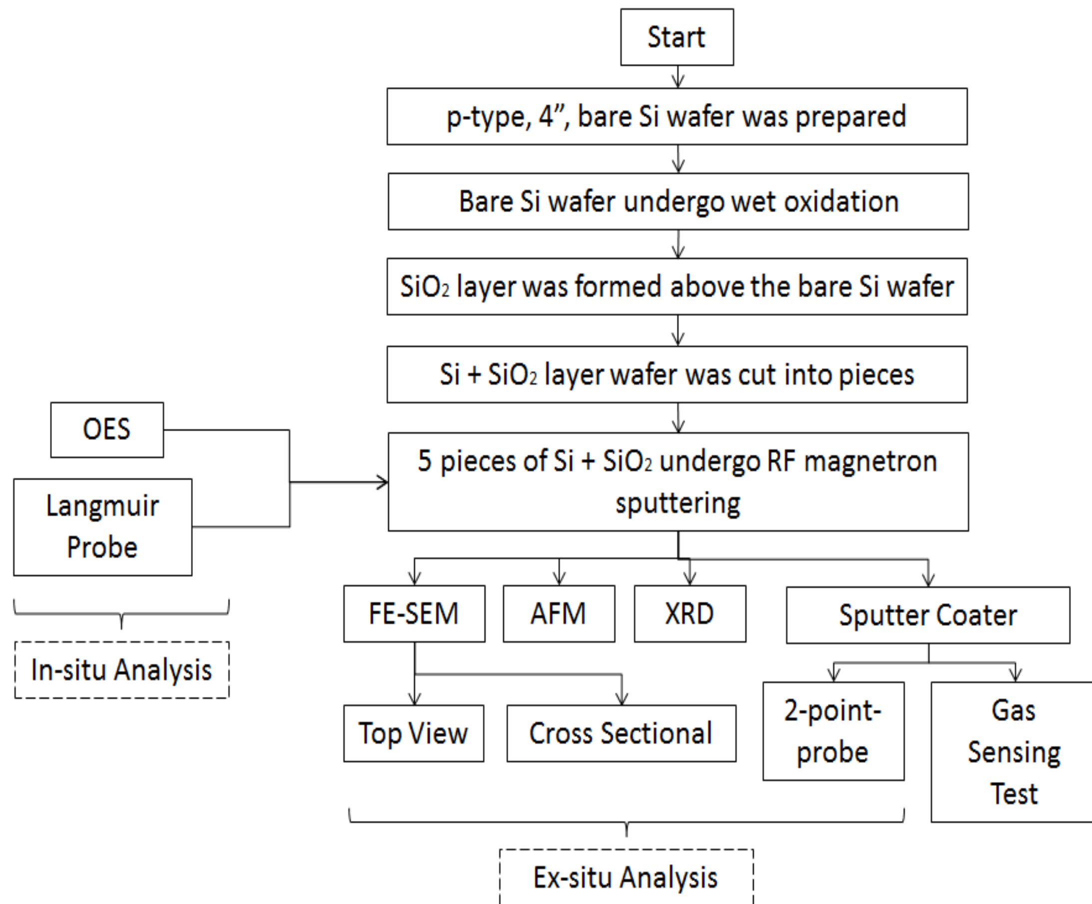

Figure 3.1: Flow chart of the process for fabricating the copper oxide gas sensor.

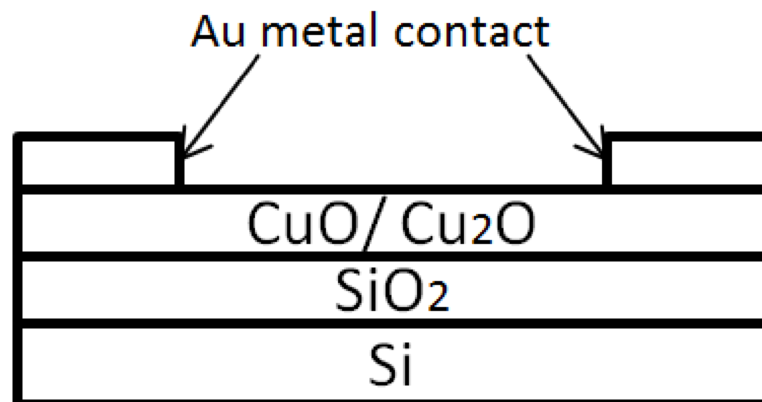

Figure 3.2: Gas sensor schematic diagram [5].

3.2 Gas sensor fabrication

In order to produce an insulator layer, the p-type Si wafer needs to undergo wet oxidation. Thermal oxidation is the most common technique utilized to produce an insulating layer. Basically, there are two types of thermal oxidation, namely dry oxidation and wet oxidation. Dry oxidation occurs when the wafer is exposed to oxygen at approximately 1000ºC. Through dry oxidation, a high quality of oxide layer will be produced. However, the dry oxidation is preferable for those that wish to produce a thin layer of oxide which is less than 0.5um. On the other hand, wet oxidation occurs when the wafer is exposed to oxygen and hydrogen at approximately 1000ºC. Thus this produces a vapour environment within the furnace. Compare to dry oxidation, wet oxidation have a higher growth rate and is much more preferable for those that wish to produce an oxide layer of 0.5um and above. Furnace is equipment that will be used in thermal oxidation as it is able to sustain temperature of over 1000ºC in the internal [39, 40]. The schematic diagram of the furnace is shown in figure 3.3. In this case, p-type Si wafer will be used and a thin layer of SiO_2 layer will be produce on top of the Si wafer. But before undergoing wet oxidation, it is common to remove organic residue from the Si wafer. In order to remove the organic residue, piranha cleaning method was used.

Piranha cleaning involves two type of acid as the solution. The acid was namely concentrated sulfuric acid (H_2SO_4) and hydrogen peroxide (H_2O_2) at a mixture of 3:1. Due to the nature of these two types of acid, the piranha clean is highly oxidative and removes metals and organics contamination. As a safety measure to handle piranha solution, only Pyrex glass containers are suitable. When preparing the piranha solution, the H_2O_2 acid was added slowly into the containers as the reaction will start immediately before the cleaning process because it produces an exothermic reaction with gas release. As a reminder, the piranha solution is very energetic and potentially explosive [41, 42]. The piranha solution will then be heated at 80°C for 20mins. By that time, the solution should begin to bubble vigorously. After that, the Si wafer will be washed with deionized water and placed inside the furnace for 4hours. Depend on the distance of the wafer from the process gas, different thickness of SiO_2 will be produced. Wafers that were placed nearer to the process gas tend to have a higher thickness of SiO_2 layer.

PTTA UTHM PERPUSTAKAAN TUNKU TUN AMINAH

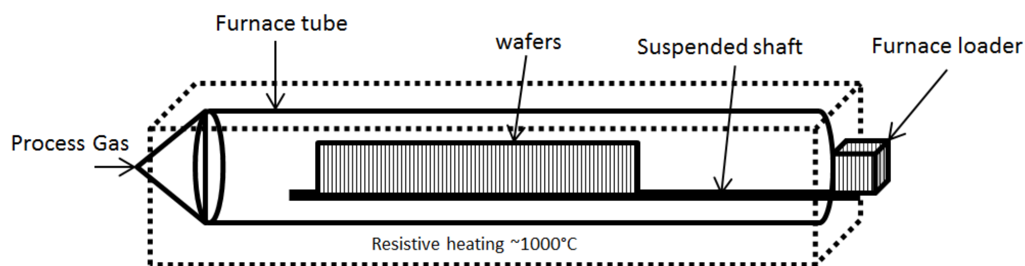

Figure 3.3: An internal view of the furnace.

As for the third layer of the gas sensor, the copper oxide thin film layer will be fabricated using magnetron sputtering. In current date, RF magnetron sputtering technique is a process to fabricate thin film. In this process, a few nanometers layers of thin films will be grown on a substrate that was initially placed inside a vacuum chamber. Through various pumping, the chamber pressures will be reduced to mTorr range and at this point plasma phase will be initiated in between the target and substrate. The main advantages of RF magnetron sputtering compared to others methods due to its low deposition rates and uniformity of the thin films [43]. Besides, RF magnetron sputtering technique is more simple and repeatability performance. Basically, since that the RF magnetron sputtering machine is an automated system, there is a system that was used to control and monitor the parameter and changes within the chamber. Through the controller system, the changes on the base pressure can be monitored and the amount of gas flow rate, dissipation power and deposition time can be easily controlled. Figure 3.4 is the schematic diagram of the RF magnetron sputtering. The magnetron sputtering mentioned in this thesis is from Nanorian Technologies with model code PSP 5004. While figure 3.5 is an illustration of the general assembly of the magnetron sputtering source [44, 45]. Depending on the parameters used the plasma within the chamber will be different. Therefore, analysis on the plasma is essential in order to better understand the plasma. Throughout this year, several diagnostic techniques were invented to analyze the plasma within the chamber. Some of the technique was namely optical emission spectroscopy (OES) and Langmuir probe. Although several diagnostic techniques has being employed to determine the plasma analysis of metal oxide [46–48], however few results are published on the plasma analysis of copper oxide through RF magnetron sputtering.

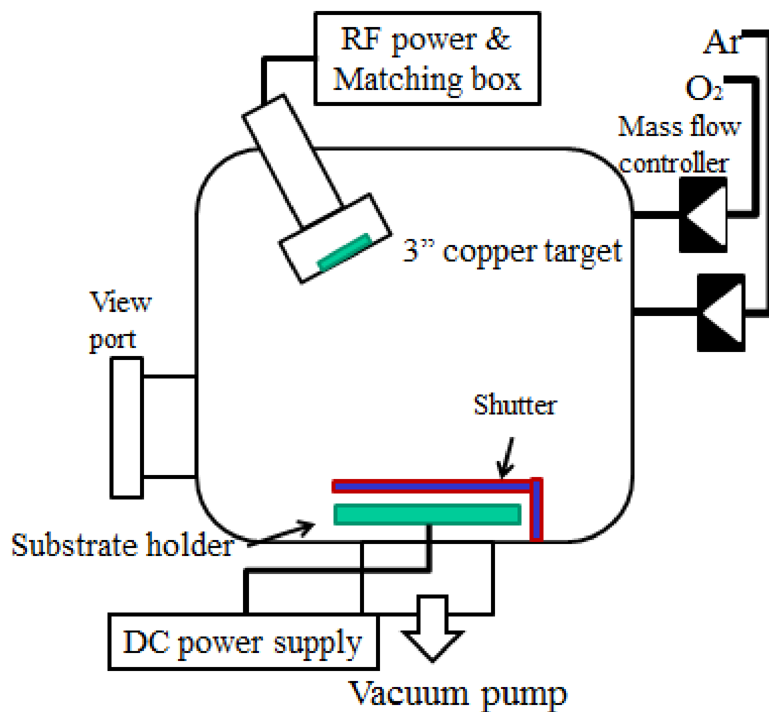

Figure 3.4: A schematic diagram of RF magnetron sputtering [45].

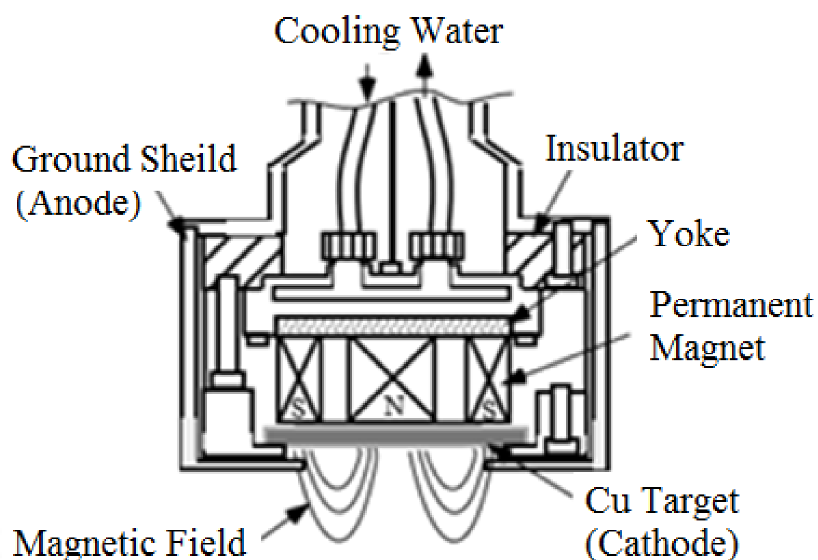

Figure 3.5: A general scheme of magnetron discharge [45].

Magnetron sputtering processes were done under vacuum base pressure, where the chamber used for sputtering process will be pumped down to vacuum base pressure of $5x10^{-6}$mTorr which required approximately above 2hours. In this part of the experiment, pure argon gas of 50sccm was admitted into the gas chamber during the deposition process. The main function of argon gas in magnetron sputtering in

this experiment was to be used as the sputter gas because argon gases tend not to react with the target material or combine with any other gases. Other gas that will be introduced is the oxygen gases that play the role as the reactive gas. For this thesis, the first parameter that was investigated was the oxygen flow rate. In this experiment, the oxygen flow rate was varied from 0sccm, 4sccm, 8sccm and 16sccm. Since that in this experiment, the properties of copper oxide plasma and thin film will be investigated. Therefore, the other main ingredient that was required in this experiment is the 3-inch high purity (99.99% purity) copper target, the reactive gas will react with the copper ions to form copper oxide thin film. The deposition time for the deposition of copper oxide thin film was set to 4minutes in order to produce copper oxide thin film with thickness of approximately 120nm. The deposition time was set based on the deposition rate of the copper oxide thin film to be approximately 29.186nm/min for 22.5mTorr working pressure and 400W dissipation power. The thickness of the copper oxide thin films prepared at 5, 10, 15 and 20minutes is shown in figure 3.6.

The substrate that were used in this experiment is a 4-inches p-type silicon wafer that have undergo wet oxidation process to form a SiO_2 layer that will act as an insulator layer. After that, the 4-inches silicon wafer will be cut into smaller pieces of 0.39x 0.79inch^2 in size.

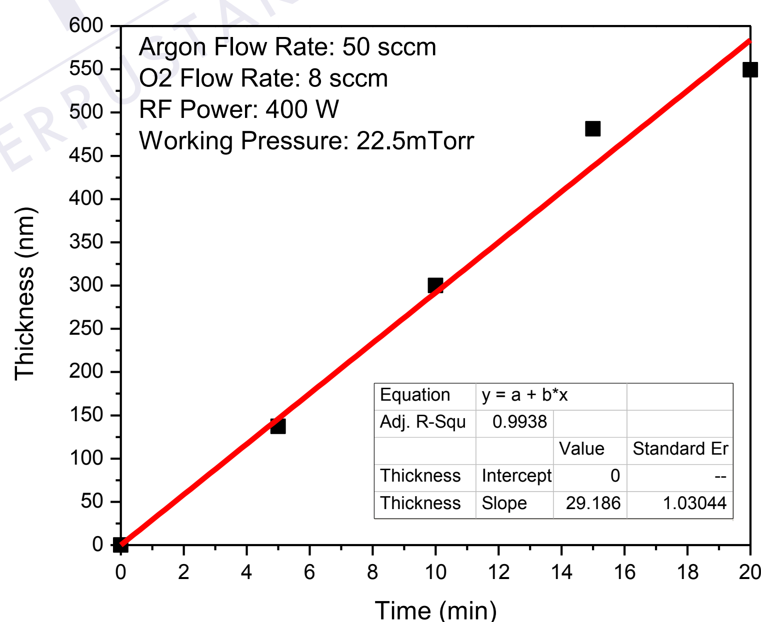

Figure 3.6: Thickness against deposition time of copper oxide thin films prepared at 5, 10, 15 and 20minutes.

PTTA UTHM PERPUSTAKAAN TUNKU TUN AMINAH

For each deposition, five pieces of the small silicon wafer will be place inside the chamber. Each piece will be used for different analysis such as field emission microscope (FE-SEM), atomic force microscope (AFM), x-ray diffraction (XRD), *I-V* characteristic and gas sensing. Besides than varying the oxygen flow rate, the substrate bias voltage were also varied by -0V, -40V, -60V and -100 V. Substrate bias voltage is the external parameter that allow the user to supply a voltage directly to the substrate. Depend on the amount of substrate bias voltage applied it will affect in the quality of the thin films deposited. The investigated deposition parameters are indicated in Table 3.1.

As for the last layer of the gas sensor, the sample is coated with a layer of gold (Au) at 40mA and 200seconds using sputter coater by JEOL JFC-1600 Auto Fine Coater as a metal contact for the two point probes experiment and gas sensing testing.

Table 3.1: The deposition conditions of the prepared copper oxide thin films.

Argon Flow Rate	50sccm
Dissipation Power	400W
Deposition Time	4minutes
Working Pressure	22.5mTorr
Substrate	Si wafer
Oxygen Flow Rate	0, 4, 8 and 16sccm
Substrate Bias Voltage	0, -40, -60 and -100V

3.3 In-situ and ex-situ analysis

Optical emission spectroscopy (OES) is a useful technique to understand the condition of the sputtering plasma without perturbing the plasma. No physical probe will be introduced into plasma. Hence, the plasma within the chamber will not be affected by the OES and the results that were obtained are accurate without contamination. As mention earlier, in order to understand the condition within the sputtering plasma OES will be used to measures the light that was emitted during sputtering process. It will measure the light emitted from the plasma in term of

PTTA UTHM PERPUSTAKAAN TUNKU TUN AMINAH

wavelength, time and location. The light that is emitted is the energy of the photons from the plasma, therefore, it have a characteristic of the composition and energy state of species within the plasma. The spectra are then used to analyze both the chemical species that make up the plasma and their state of excitation. Basically, OES is a technique used to monitor the chemical species that was build up in various plasma conditions. It can be used to investigate the emissive species within the plasma, since at different plasma condition the amount of emissive species in the plasma will be different. Hence, it will contribute significantly to the properties of the thin film produced [47]. Optical emission measurement were usually made through the window on the plasma chamber, with a monochromatic system the measures the plasma in the range of 200nm to 1000nm wavelength [49]. The proper configuration to use an OES device is by connecting the HR4000 to a personal computer that were installed with software named spectra suite. With this software, it allows the user to communicate with the HR4000 and allowed it to extract information from the plasma. Besides than a personal computer, the HR4000 will also be connected to an optical fiber that was used as a medium to extract the information from the plasma. Besides than the optical fiber, an optical lens was placed in between the optical fiber and the chamber in order to focus the extraction point of the OES at a single point which is 2cm above the substrate and 11cm from the copper target. Of course, a simple experimental test will be conducted in order to confirm the actual position that will be used as the extraction point. The simple experimental test was by using the OES to focus on a laser point that was shoot out from a known laser sources with wavelength of 632.8nm. The result of the simple experimental test was plotted into figure 3.7. Figure 3.7 is the intensity of the He-Ne laser radiation that was observed by the OES. While figure 3.8 is the actual result that was obtain directly from the Ocean Optic Spectra Suite software. A schematic diagram of the magnetron sputtering embedded with optical emission spectroscopy was displayed in figure 3.9.

PTTA UTHM PERPUSTAKAAN TUNKU TUN AMINAH

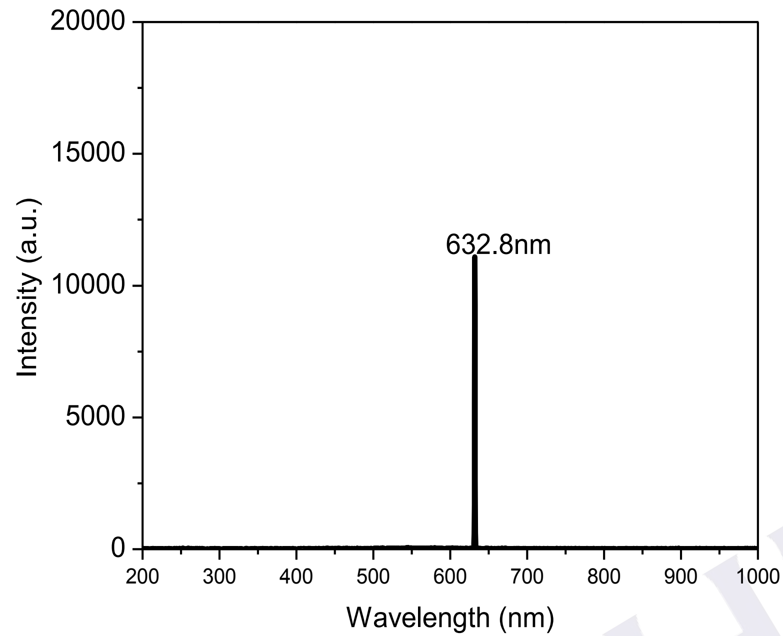

Figure 3.7: The OES result for the He-Ne laser radiation.

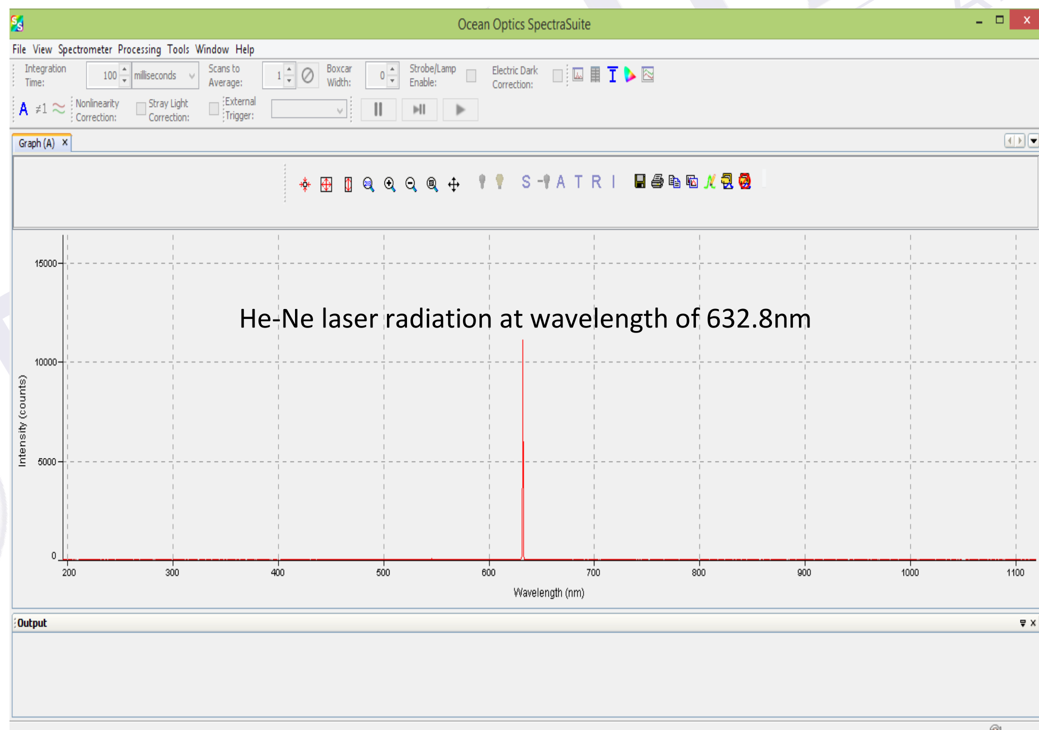

Figure 3.8: The actual result obtainable from the Ocean Optics Spectra Suite software.

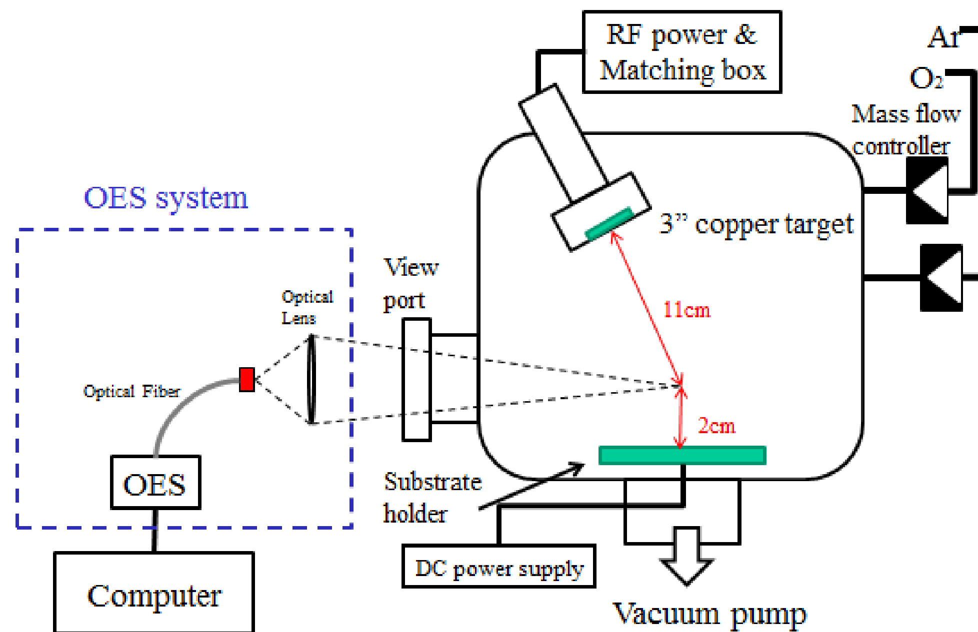

Figure 3.9: RF magnetron sputtering embedded with OES [45].

On the other hand, a Langmuir probe is a small conductor that is introduced into the plasma in order to collect the ion or electron current that flow to it in response to different voltages. Through Langmuir probe, the current versus voltage curve will be obtain and analysis is done to obtain the information about the plasma potential (V_p), electron temperature (T_e), deybe length (λ_D), ion density (n_i), electron density (n_e) and ion flux. In order to protect the probe and to ensure the circuitry to give the correct *I-V* curves, a special technique is used to make the probe tip. The probe tip is made of a high temperature material, usually tungsten rod with 5micron in diameter and 3.2cm in length. To avoid the probe tip from disturbing the plasma, the ceramic tube is made into as thin as possible of less than 1mm in diameter. The probe will be inserted into the RF magnetron sputtering through the side view port. The probe tip will be position 2cm from the substrate and 11cm from the target. The commercially available Langmuir probe is ESPION Advanced Langmuir Probe from Hiden Analytical. An illustration of the probe tip design and the full system is shown in figure 3.10 and figure 3.11, respectively [50]. Through the Hiden Analytical software, there are two variables that will be set at the beginning of the experiment. The two variables are the atomic mass unit of the primary gas used and the probe surface area. Since that the primary gas used in the magnetron sputtering discharge were argon gas, the molecular weight in this case were set to 40a.m.u. As

for the surface area of the tip, it was set as 4.73mm^2. Figure 3.12 display part of the setting available in the Hiden Analytical Software Suite. While Figure 3.13 shows the appearances of the Hiden Analytical Software Suite before analyzing the result.

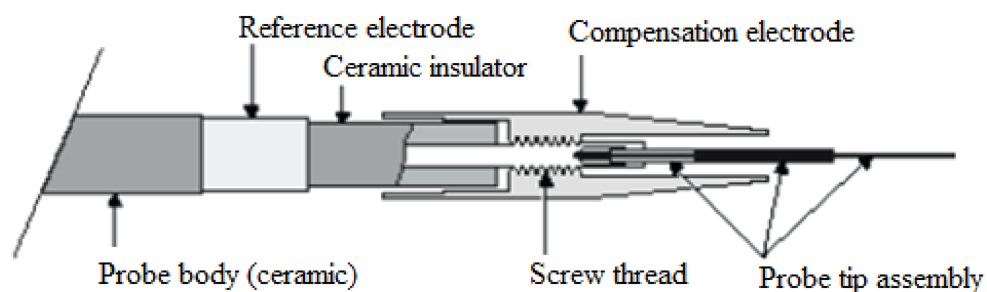

Figure 3.10: Probe tip assembly in the Hiden Analytical ESPion system [50].

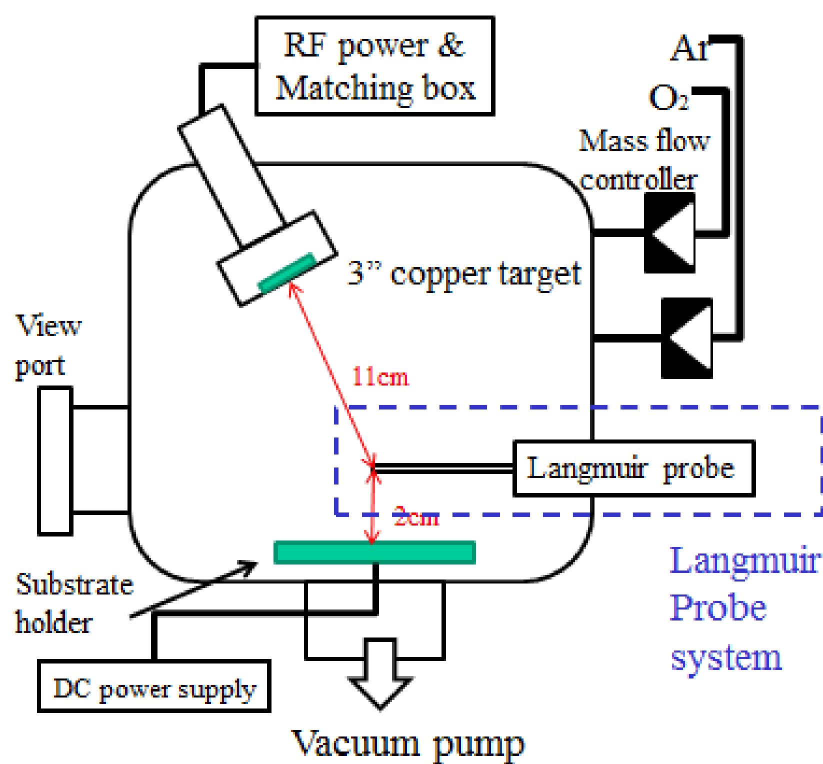

Figure 3.11: RF magnetron sputtering embedded with Langmuir probe [45].

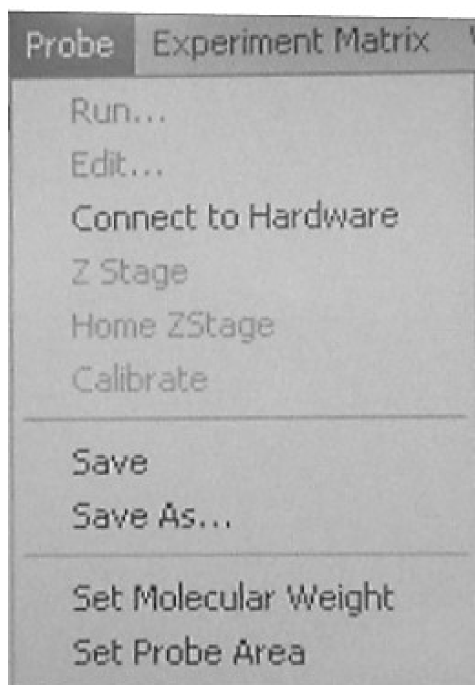

Figure 3.12: The initial variable setting available in the Hiden Analytical Software Suite.

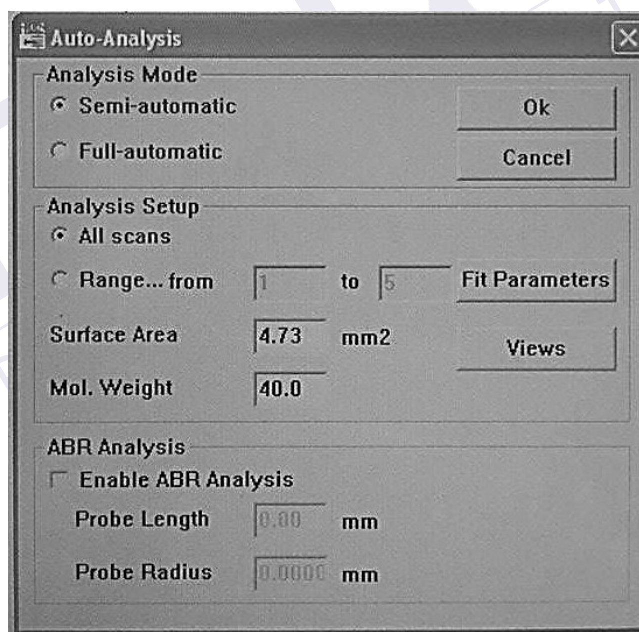

Figure 3.13: The appearances of the Hiden Analytical Software Suite before analysis.

As we know, physical properties of the sputtered copper oxide thin films are controlled by its surface structure, which are influenced by the energy of ion bombardment towards the substrate. Therefore, the effect of plasma condition towards the formation of thin films is important. Though the plasma conditions are

controlled by several parameters such as gas flow rate, working pressure, dissipation power and substrate bias voltage. In recent years, there have being reports of some interesting work based on this copper oxide material prepared using various techniques. However, some of the common physical properties analysis method includes X-Ray Diffraction (XRD), Field Emission Scanning Electron Microscope (FE-SEM), Transmission Electron Microscopy (TEM), UV-Vis Spectrometer and Atomic Force Microscope (AFM). Based on the analysis, most of the gas sensing material that were investigated by several researchers shows that the grain size of the copper oxide thin films produced is less than 100nm [6,19,22]. While there are various peaks of Cu, Cu_2O and CuO was detected using XRD analysis. Even though there have being various evaluations on the physical properties of copper oxide thin films, none was commenting on the correlation of the plasma condition and the physical properties of copper oxide thin films. Therefore, the aim for this thesis is to understand the correlation between plasma condition and physical properties towards the gas sensing performance.

In this thesis, Field Emission Scanning Electron Microscope (FE-SEM), Atomic Force Microscope (AFM) and X-Ray Diffraction (XRD), will be used. FE-SEM is a type of instrument that produces image of a sample by scanning it with a focused beam of electrons. These electrons will interact with the atoms in the sample, producing various signal that can be detected and contain information about the sample's topography and composition. Basically, these electrons are liberated from a field emission source and accelerated in a high electrical field gradient. This field emission source is composed from metal with high melting point, such as tungsten. The metal shape is very sharp to produce a very fine electron beam. In order to focus the electron beam onto the sample, the scanning is done under high vacuum condition which is less than 10^{-4}Pa. Other than that, the primary electrons are focused and deflected by using electronic lenses to narrow down the beam so that it will only scan on a specific area of the sample as shown in figure 3.14. Upon contact of the primary electron with the sample, a secondary electron is emitted from each spot of the sample. A detector catches the secondary electron and produce electronic signal. Depending on the angle and velocity of the secondary electrons, it is often relate to the surfaces structure of an object. The signal received is then amplified and transformed into a video scan image that can be seen at monitor [51]. A photograph of the schematic diagram of FE-SEM is shown in figure 3.14.

PTTA UTHM PERPUSTAKAAN TUNKU TUN AMINAH

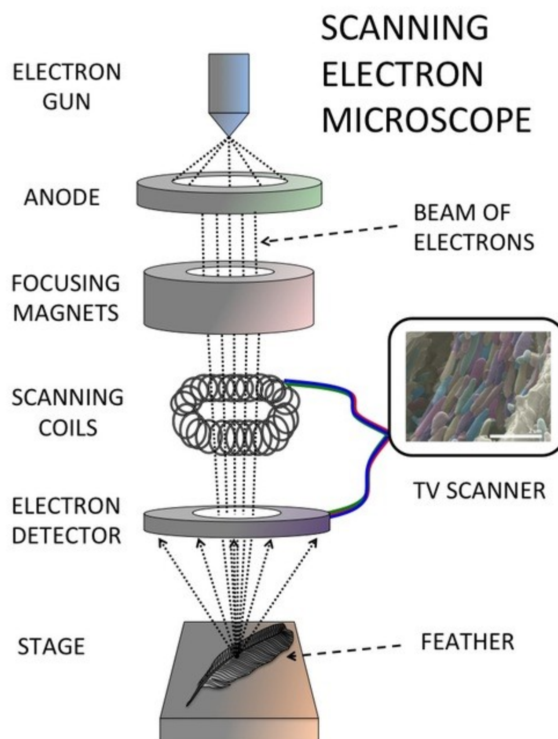

Figure 3.14: FE-SEM schematic diagram [52]

Atomic force microscope (AFM) is a very high-resolution type of scanning probe microscopy that able to measure the three dimensional topography and physical properties of a surface with a sharpened probe. The probe, which is also called cantilever, is less than 50nm in diameter and the areas scanned by the probe are less than 100um. AFM consist of three types imaging modes, the contact mode, non-contact mode and tapping mode. Typically, contact mode means that the probe will interact with the surface of the object as it scanned through it. Likewise, non-contact mode means that the probe is positioned a few nanometers from the sample surface. In this project, the non-contact mode was used. In non-contact mode, the probe will not touch the surface as it scanned through the surface of the object. Therefore, the cantilever used in non-contact mode is a non-contact cantilevers. It has a tip radius of curvature to be less than 10nm. Identical to the non-contact mode, tapping mode also positioned close enough to the surface. The only different is that, in tapping mode the probe is driven to oscillate up and down at near its resonance frequency as it scanning through the surface of the object. In order to acquire the image, the AFM can generally measures the vertical and lateral deflections of the probe by using optical lever. The optical lever functions by reflecting the laser beam

REFERENCES

1. Bochenkov, V. E. & Sergeev, G. B. (2010). Sensitivity , Selectivity , and Stability of Gas-Sensitive Metal-Oxide Nanostructures. *American Scientific Pubishers*, 3, pp. 31–52.

2. Wang, C., Yin, L., Zhang, L., Xiang, D. & Gao, R. (2010). Metal oxide gas sensors: sensitivity and influencing factors. *Sensors*, 10, pp. 2088–2106.

3. Korotcenkov, G. (2007). Metal oxides for solid-state gas sensors: What determines our choice? *Mater. Sci. Eng. B,* 139, pp. 1–23.

4. Park, J. (2010). Nanostructured semiconducting metal oxides for use in gas sensors. *Doctor of Philosophy thesis, Institute for Superconducting and Electronic Materials, University of Wollongong.*

5. Parmar, M. & Rajanna, K. (2011). Copper (II) oxide thin film for methanol and ethanol sensing. *Int. J. on Smart Sensing and Intelligent Systems*, 4(4), pp. 710–725.

6. Figaro, "General information for tgs sensors," Retrieved Dec 14, 2014, from http://www.figarosensor.com/products/general.pdf.

7. Chowdhuri, A., Sharma, P., Gupta, V., Sreenivas, K., and Rao, K. P. (2002). H_2S gas sensing mechanism of SnO_2 films with ultrathin CuO dotted islands, *J. Appl. Phys.*, 92(4), pp. 2172-2180.

8. Liu, J., Huang, X., Liu, W., Jiao, Z., Chao, W., and Yu, Z. (2003). H_2S Detection Sensing Characteristic of CuO/SnO_2 Sensor. 3, pp. 110-118.

9. Jun, S. T. and Choi, G. M. (1994). CO gas-sensing properties of ZnO/CuO contact ceramics. *Sensors Actuators B Chem.*, 17(3), pp. 175–178.

PTTA UTHM PERPUSTAKAAN TUNKU TUN AMINAH

10. Yang, C., Su, X., Wang, J., Cao, X., Wang, S. and Zhang, L. (2013). Facile microwave-assisted hydrothermal synthesis of varied-shaped CuO nanoparticles and their gas sensing properties. *Sensors Actuators B. Chem.*, 185, pp. 159–165.

11. Papadimitropoulos, G., Vourdas, N., Vamvakas, V. E. and Davazoglou. D., (2005). Deposition and characterization of copper oxide thin films. *J. Phys. Conf. Ser.*, 10, pp. 182–185.

12. Barreca, D. *et al.* (2009). Chemical vapor deposition of copper oxide films and entangled quasi-1D nanoarchitectures as innovative gas sensors. *Sensors Actuators B Chem*., 141, pp. 270–275.

13. Johan, M. R., Shahadan, M., Suan, M., Hawari, N. L. & Ching, H. A. (2011). Annealing Effects on the Properties of Copper Oxide Thin Films Prepared by Chemical Deposition. *Int. J. Electrochem. Sci*., *6*, pp. 6094–6104.

14. Zhang, Y., He, X., Li, J., Zhang, H. & Gao, X. (2007). Gas-sensing properties of hollow and hierarchical copper oxide microspheres. *Sensors Actuators B Chem*., 128, pp. 293–298.

15. C. Yang, X. Su, F. Xiao, J. Jian, and J. Wang. (2011). Gas sensing properties of CuO nanorods synthesized by a microwave-assisted hydrothermal method. *Sensors Actuators B Chem.,* 158(1), pp. 299–303.

16. Samarasekara, P., Kumara, N. T. R. N. & Yapa, N. U. S. (2006). Sputtered copper oxide (CuO) thin films for gas sensor devices. *J. Phys. Condens. Matter*, 18, pp. 2417–2420.

17. Zoolfakar, A. S. *et al.* (2013). Nanostructured copper oxides as ethanol vapour sensors. *Sensors Actuators B Chem*., 185, pp. 620–627.

18. Technologies, A. Q. Complete list of VOC ' s. Retrieved Dec 14, 2014, from *http://www.aqt.it/index.php?option=com_content&view=article&id=71&Itemid=107*, pp. 1–20, 2014.

PTTA UTHM PERPUSTAKAAN TUNKU TUN AMINAH

19. Weber, I. T., Andrade, R., Leite, E. R. and Longo, E. (2001). A study of the $SnO_2.Nb_2O_5$ system for an ethanol vapour sensor : a correlation between microstructure and sensor performance. *Sensors Actuators: B. Chem*. 72, pp. 180–183.

20. Pawar, N. K., Kajale, D. D., Patil, G. E., Wagh, V. G., Gaikwad, V. B., Deore, M. K., Jain, G. H. and Mig, O. (2012). Nanostructured Fe_2O_3 thick film as an ethanol sensor. *Int. J. on Smart Sensing and Intelligent Systems.* 5(2), pp. 441–457.

21. T. Joseph and M. Morrison. (2006). Nanotechnology in Agriculture and Food. *Institute Nanotechnol.*, pp. 1-13.

22. E. Mostafa and W. Buescher. (2011). Indoor air quality improvement from particle matters for laying hen poultry houses. *Biosyst. Eng.*, 109(1), pp. 22–36.

23. Lee. K. K. (2013). China lifts ban on Malaysian birds' nest import. *New Straits Times*.

24. Rosli Ilham. (2012). 24 Petronas workers hurt in gas leak. *New Straits Times*.

25. Ho, S. and Foong, J. (2009). Six die of ammonia poisoning. *The Star*.

26. Chapter 4 Solid-State Gas Sensors. *International Sensor Technology*, *pp.* 47–53. Retrieved May 14, 2014, from http://intlsensor.com/pdf/solidstate.pdf.

27. Hwang, I. S., Choi, J. K., Kim, S. J., Dong, K. Y., Kwon, J. H., Ju, B. K. and Lee, J. H. (2009). Enhanced H_2S sensing characteristics of SnO_2 nanowires functionalized with CuO. *Sensors Actuators B Chem.*, 142(1), pp. 105–110.

28. Sohn, J. C., Kim, S. E., Kim, Z. W. and Yu, Y. S. (2009). H_2S Gas Sensing Properties of SnO_2:CuO Thin Film Sensors Prepared by E-beam Evaporation. *Trans. Electr. Electron. Mater.*, 10(4), pp. 135–139.

29. Bahu, M., Kishor, K, and Tanveer, Bahu. (2012). CuO-ZnO semiconductor gas sensor for ammonia at room temperature. *J. Electron Devices*, 14, pp. 1137–1141.

PTTA UTHM
PERPUSTAKAAN TUNKU TUN AMINAH

30. Corpuz, R. D. and Albia, J. R. (2014). Electrophoretic Fabrication of ZnO / ZnO-CuO Composite for Ammonia Gas Sensing. *Mater. Res.*, 17(4), pp. 851–856.

31. Liao, L. *et al* (2009). Multifunctional CuO nanowire devices: p-type field effect transistors and CO gas sensors. *Nanotechnology*, 20, pp. 1-6.

32. Aslani, A. and Oroojpour, V. CO gas sensing of CuO nanostructures, synthesized by an assisted solvothermal wet chemical route. *Phys. B Condens. Matter*, 406(2), pp. 144–149.

33. Nemade, K. R. and Waghuley, S. A. Optical and Gas Sensing Properties of Cuo Nanoparticles Grown by Spray Pyrolysis of Cupric Nitrate Solution. (2014). *Int. J. Mater. Sci. Eng.*, 2(1), pp. 63–66.

34. Gu, H., Wang, Z. and Hu, Y. (2012). *Hydrogen Gas Sensors Based on Semiconductor Oxide Nanostructures*. 12, pp. 5517–5550.

35. Mark. (2010). History of PVD coatings. pp. 1-5. Retrieved April 24, 2014, from http://www.pvd-coatings.co.uk/history-pvd-coatings/.

36. Shizuka, S. I., Aruyama, T. M. & Kimoto, K. A. (2000). Thin-Film Deposition of Cu_2O by Reactive Radio-Frequency Magnetron Sputtering. *Jpn. J. Appl. Phys.*, 39, pp. 786–788.

37. Developed by IEEE. Insulators and Conductors. *TryEngineering*, pp. 1–9. Retrieved May 14, 2014, from http://tryengineering.org/lessons/insandcond.pdf.

38. Chapter 4: Conductors and Insulators. pp. 29–32. Retrieved May 14, 2014, from http://www.kitbook.com/uploads/file/ECK%20te%20chapter%204.pdf.

39. Cheung, P. N. & Berkeley, U. C. Thermal Oxidation of Si. *Lecture Note.* Retrieved May 14, 2014, from https://www.eng.tau.ac.il/~yosish/courses/vlsi1/I-4-1-Oxidation.pdf.

PTTA UTHM PERPUSTAKAAN TUNKU TUN AMINAH

40. Exercise 1. Thermal oxidation of silicon wafers . Ellipsometric measurement of oxide thickness . *Fundam. Microtechnology Lab*, pp. 1–5. Retrieved May 14, 2014, from http://www.dsod.p.lodz.pl/materials/PP0201_IFE.pdf.

41. Piranha Clean. Retrieved May 14, 2014, from http://www.engr.ucsb.edu/~memsucsb/Facilities/mems%20fab/PIRANHA%20CLEAN.pdf.

42. Mak, P. (2010). Piranha Clean Procedure. *Boston Uni. Photonics Center*, pp 1-3. Retrieved May 14, 2014, from http://www.bu.edu/photonics/files/2011/02/Piranha_clean.pdf.

43. Hari Prasad Reddy, M., Sreedhar, A. & Uthanna, S. (2012). Structural, surface morphological and optical properties of nanocrystalline Cu_2O films prepared by RF magnetron sputtering: substrate bias effect. *Indian J. Phys.* 86(4), pp. 291–295.

44. Kashtanov, P. V., Smirnov, B. M. & Hippler, R. (2007). Magnetron plasma and nanotechnology. *Russ. Acad. Sci*., 50(5), pp. 455-458.

45. Nayan, N. Bin. (2008). Studies on high – pressure magnetron sputtering plasmas using laser – aided diagnostic techniques. *Grad. Shool Eng. Nagoya Univ.*

46. Kim, Y. (2005). Optical Emission Spectroscopy During RF Magnetron Sputtering of Y_2O_3, Ba , Cu , and $YBa_2Cu_3O_{7-x}$ Targets under Argon and Oxygen Atmospheres. 46(4), pp. 926–930.

47. Bang, S. B., Chung, T. H. & Kim, Y. (2003). Plasma enhanced chemical vapor deposition of silicon oxide films using TMOS/O_2 gas and plasma diagnostics. *Thin Solid Films*, 444, pp. 125–131.

48. Pintaske, R. *et al.* (1998). Spectroscopic studies of a magnetron sputtering discharge for boron nitride deposition. *Surface and Coatings Tech*., *99*, pp. 266–273.

PTTA UTHM PERPUSTAKAAN TUNKU TUN AMINAH

49. Chang, J. P. (2002) Principles of Plasma Processing. *Course Notes*, pp. 151–166.

50. Chen, F. F. (2003). Lecture Notes on Langmuir Probe Diagnostics. *IEEE-ICOPS Meet.* pp. 1-40.

51. Janseen, G. Information on the FESEM (Field-emission Scanning Electron Microscope). *Radboud Universiteit Nijmegan*. Retrieved May 14, 2014, from http://www.vcbio.science.ru.nl/public/pdf/fesem_info_eng.pdf.

52. Prehistoric colours. (2013). Magnification Machines. pp. 1–3. Retrieved May 14, 2014, from http://prehistoric-colours.tumblr.com/post/53189877826/magnification-machines.

53. Atomic force microscopy. pp. 1–12. Retrieved May 14, 2014, from http://web.stevens.edu/nue/about.html.

54. Mai, W. Fundamental Theory of Atomic Force Microscopy by Wenjie Mai. Retrieved May 14, 2014, from http://www.nanoscience.gatech.edu/zlwang/research/afm.html.

55. Zur, H. L. X-Ray Diffraction HOW IT WORKS. *Univ. South Carolina*. Retrieved May 14, 2014, from http://www.chem.sc.edu/faculty/zurloye/XRDTutorial_2013.pdf.

56. Tovborg, A. J. (1943). Determination of particle size by the x-ray powder method," *Kobenhavn*, pp. 1-10.

57. Brennan, R. & Dickey, D. Determination of Diffusion Characteristics Using Two- and Four-Point Probe Measurements. *Sloecon Labs Tech.* pp. 1–10.

58. Peyronel, M. & Marangoni, A. (2014). Analytical Methods , Procedures and Theory for the Physical Characterization of Fats Section 1 : X-Ray Powder Diffractometry. Retrieved May 14, 2014, from http://lipidlibrary.aocs.org/physics/xray/index.htm.

PTTA UTHM PERPUSTAKAAN TUNKU TUN AMINAH

59. Koirala, S. P., Abu-safe, H. H., Mensah, S. L., Naseem, H. A. & Gordon, M. H. (2008) . Langmuir probe and optical emission studies in a radio frequency (rf) magnetron plasma used for the deposition of hydrogenated amorphous silicon. *Surf. Coatings Technol.* 203, pp. 602–605.

60. Tsaneva, V. N., Popov, T. K., Dias, F. M., Tarte, E. J. & Blamire, M. G. (2003). Optical emission spectroscopy and Langmuir probe characterisation of the plasma during high-pressure sputter deposition of high-T_c superconducting $YBa_2Cu_3O_{7-x}$ thin films. *Vacuum*, 69, pp. 261–266.

61. Acosta, J., Rojo, A., Salas, O. & Oseguera, J. (2007). Process monitoring during AlN deposition by reactive magnetron sputtering. *Surf. Coatings Technol*., 201, pp. 7992–7999.

62. Hanif, M., Salik, M. & Baig, M. A. (2011). Quantitative studies of copper plasma using laser induced breakdown spectroscopy. *Opt. Lasers Eng*., 49, pp. 1456–1461.

63. Lien, S.-Y. *et al.* (2011). Characterization of HF-PECVD a-Si:H thin film solar cells by using OES studies. *J. Non. Cryst. Solids*, 357, pp. 161–164.

64. Ogwu, A. A. *et al.* (2005). An investigation of the surface energy and optical transmittance of copper oxide thin films prepared by reactive magnetron sputtering. *Acta Mater*., 53, pp. 5151–5159.

65. Mugwang'a, F. K., Karimi, P. K., Njoroge, W. K., Omayio, O. & Waita, S. M. (2013). Optical characterization of Copper Oxide thin films prepared by reactive dc magnetron sputtering for solar cell applications. *Int. J. Thin Film. Sci. Technol*., 2(1), pp. 15–24.

66. Muthe, K. . *et al.* (1998). A study of the CuO phase formation during thin film deposition by molecular beam epitaxy. *Thin Solid Films*, 324, pp. 37–43.

67. Lim, J., Ishikawa, Y., Miyake, K., Yamashita, M. & Isshiki, M. (2002). Influence of Substrate Bias Voltage on the Properties of Cu Thin Films by

PTTA UTHM PERPUSTAKAAN TUNKU TUN AMINAH

Sputter Type Ion Beam Deposition. *Materials Transactions*, 43(6), pp. 1403–1408.

68. Sputtering. Retrieved May 14, 2014, from Http://users.wfu.edu/ucerkb/Nan242/L07-Sputtering_a.pdf.

69. Park, J., Lim, K., Ramsier, R. D. & Kang, Y. (2011). Spectroscopic and Morphological Investigation of Copper Oxide Thin Films Prepared by Magnetron Sputtering at Various Oxygen Ratios. *Bull. Korean Chem. Soc.* 32(9), pp. 3395–3399.

70. Ogwu, A. A. (2007). Electrical resistivity of copper oxide thin films prepared by reactive magnetron sputtering. *J. Achiev. Mater. Manucafturing Eng.*, 24(1), pp. 172–177.

71. Hiden Analytical. Plasma Diagnostics – Plasma Characterisation Using a Langmiur Probe by Hiden Analytical. Retrieved May 14, 2014, from Http://www.azom.com/article.aspx?ArticleID=4169#_What_is_Langmuir.

72. Brockhaus, A., Schwabedissen, A., Soll, C. & Engemann, J. Electron Density Measurements in a Microwave Plasma by the Plasma Oscillation Method. pp. 1–4. Retrieved May 14, 2014, from https://crppwww.epfl.ch/LTPD99/pdf/orals/Brockhaus.pdf.

73. Ghasemi, S., Ghomi, H. R., Niknam, A. R. & Latifi, H. (2013). Investigation of Influence of Gas Ratio on the Electron Temperature in TiN Magnetron Sputtering Deposition System. *Int. Conf. Phenom. Ioniz. Gases*, pp. 1–3.

74. Yoon, J. S. & Han, J. G. (1997). The ion current density and spectroscopic study in a straight magnetic filtering arc deposition system. *Surf. Coatings Technol.* 94-95, pp. 201–206.

75. Araghi, F. & Dorranian, D. (2013). Effect of negative ions on the characteristics of plasma in a cylindrical discharge. *J. Theor. Appl. Phys.* 7(41), pp. 1-8.

PTTA UTHM PERPUSTAKAAN TUNKU TUN AMINAH

76. Knizhnik, K. Derivation of the plasma debye length. Retrieved May 14, 2014, from http://www.pha.jhu.edu/~kknizhni/Plasma/Derivation_of_Debye_Length.pdf.

77. Kaltofen, R., Sebald, T. & Weise, G. (1997). Low-energy ion bombardment effects in reactive rf magnetron sputtering of carbon nitride films. *Thin Solid Films*, 308-309, pp. 118–125.

78. Hurkmans, T., Lewis, D. B., Paritong, H., Brooks, J. S. & Mu, W. D. (1999). Influence of ion bombardment on structure and properties of unbalanced magnetron grown CrN_x coatings. *Surface and Coatings Technology*, 114, pp. 52–59.

79. (2002). Class notes for EE5383/Phys 5383. pp. 1–19. Retrieved May 14, 2014, from http://www.utdallas.edu/~goeckner/plasma_tech_class/PlasmaTech%20Sheaths_probes.doc.

80. Liu, X. & Li, D. (2006). Influence of charged particle bombardment and sputtering parameters on the properties of HfO_2 films prepared by dc reactive magnetron sputtering. *Appl. Surf. Sci.*, 253, pp. 2143–2147.

81. Orikasa, Y. , Hayashi, N. and Muranaka, S. (2008). Effects of oxygen gas pressure on structural, electrical, and thermoelectric properties of $(ZnO)_3In_2O_3$ thin films deposited by rf magnetron sputtering. *J. Appl. Phys.*, 103(11), pp. 1-7.

82. Meng, L. J. and Dos Santos, M. P. (1993). The influence of oxygen partial pressure on the properties of DC reactive magnetron sputtered titanium oxide films. pp. 319–325.

83. Oliveira, R. R. L. De, Albuquerque, D. A. C. & Cruz, T. G. S. (2012). Measurement of the Nanoscale Roughness by Atomic Force Microscopy : Basic Principles and Applications. *www.intechopen.com*, pp. 147–175.

PTTA UTHM PERPUSTAKAAN TUNKU TUN AMINAH

84. Lee, H. *et al.* (2003). Rapid Thermal Annealing Treatment of Electroplated Cu Films. *J. Korean Phys. Soc.* 43(5), pp. 841–846.

85. Morales, J., Sánchez, L., Martín, F., Ramos-Barrado, J. R. & Sánchez, M. (2004). Nanostructured CuO thin film electrodes prepared by spray pyrolysis: a simple method for enhancing the electrochemical performance of CuO in lithium cells. *Electrochim. Acta*, 49, pp. 4589–4597.

86. Yu, T., Zhao, X., Shen, Z. ., Wu, Y. . & Su, W. (2004). Investigation of individual CuO nanorods by polarized micro-Raman scattering. *J. Cryst. Growth*, 268, pp. 590–595.

87. Szil, E., Horv, Z. E., Pet, G., Lohner, T. & Moln, G. L. (1999). Enhancement of oxidation resistance in Cu and Cu (Al) thin layers. *Nucl. Instruments Methods Phys. Res. B*, 148, pp. 868–871.

88. Dow, W., Wang, Y. & Huang, T. (2000). TPR and XRD studies of yttria-doped ceria / gamma-alumina-supported copper oxide catalyst. *Appl. Catal. A Gen.*, 190, pp. 25–34.

89. Manoj, D., Ranjith Kumar, D. & Santhanalakshmi, J. (2012). Impact of CuO nanoleaves on MWCNTs/GCE nanocomposite film modified electrode for the electrochemical oxidation of folic acid. *Appl. Nanosci.* 2, 223–230.

90. Reddy, A. S., Venkata Rao, G. , Uthanna, S. and Sreedhara Reddy, P. (2005). Influence of substrate bias voltage on the properties of magnetron sputtered Cu2O films. *Phys. B Condens. Matter*, 370(1–4), pp. 29–34.

91. Ma, Y. *et. al.* (2002). Study on Sensitivity of Nano-Grain ZnO Gas Sensors. *J. Wide Bandgap Mater.*, 10(2), pp. 113–120.

92. Sun, Y. F., Liu, S. B., Meng, F. L., Liu, J. Y., Jin, Z., Kong, L. T. and Liu, J. H. (2012). Metal oxide nanostructures and their gas sensing properties: a review.," *Sensors (Basel).*, 12, pp. 2610–2631.

PTTA UTHM PERPUSTAKAAN TUNKU TUN AMINAH